# How the addition of atomic hydrogen to a multiple bond can be catalyzed by water molecules

Patrick Chaquin, Franck Fuster, Alexis Markovits

# How the addition of atomic hydrogen to a multiple bond can be catalyzed by water molecules

Patrick Chaquin[1], Franck Fuster[1], Alexis Markovits*[1]

Sorbonne Université, Laboratoire de Chimie Théorique, UMR 7616 CNRS, 75005, Paris, France

*Corresponding author

Email address: alexis.markovits@sorbonne-universite.fr

## Abstract

Observational data show complex organic molecules in the Interstellar Medium (ISM). Hydrogenation of small unsaturated carbon double bond could be one way for molecular complexification. It is important to understand how such reactivity occurs in the very cold and low-pressure ISM. Yet, there is water ice in the ISM, either as grain or as mantle around grains. Therefore, the addition of atomic hydrogen on double-bonded carbon in a series of seven molecules have been studied and it was found that water catalyses this reaction. The origin of the catalysis is a weak charge transfer between the $\pi$ MO of the unsaturated molecule and H atom, allowing a stabilizing interaction with $H_2O$. This mechanism is rationalized using the Non-Covalent Interaction and the Quantum Theory of Atoms In Molecules approaches.

Keywords: hydrogenation; Complex Organic Molecules; NCI; QTAIM

## 1. Introduction

As observation of the interstellar medium (ISM) has improved, so have the number and complexity of molecules discovered[1]. One of the key questions is how Chemistry in an environment such as the MIS could lead to molecular complexification. Indeed, despite the extremely low temperature and very low density of the reagents, complex organic molecules (Coms) were formed. One possible route is the hydrogenation of unsaturated molecules. To enable this reactivity, heterogenous

catalysis on grains could be one of the explanations[2]. In the ISM, water ice could play a particularly important role[3]. As well as being present as grains, they often form a mantle around other solids. Many theoretical works have been carried with water ice models: see[4], [5] and references therein. For instance, small water clusters have been used with DFT methods[6] or post Hartree-Fock methods[7] to calculate interaction energies with interstellar species. With larger water molecules cluster and DFT methods, formamide, acetaldehyde, glycine synthesis and CO hydrogenation have been studied [8]–[11]. Binding energies of several molecules with amorphous or cristalline solid water have been calculated with models taking into account periodicity of the solid (slab models)[12]. With the help of a computer procedure using the semiempirical GFN2 tight-binding method and the GFN-FF force field method, Germain et al.[5] build-up several very large water ice clusters to evaluate the interaction energy with $NH_3$. Despite extensive experimental and theoretical work on the effect of water ice on the reactivity of unsaturated molecules, the mechanism by which water ice acts as a catalyst remains to be understood.

In this paper, we will present a possible mechanism allowing a significant lowering by water molecules of the energy barrier in the addition of $H^{\cdot}$ on carbon atom in some multiple bonds. The origin of the phenomenon will be first presented on the example of ethylene and one water molecule. Then the results of H addition on a panel of multiple bonds will be compared and discussed on the basis of topological analyses on the various interactions of the species of concern. Finally, the effect of small cluster water molecules will be studied.

## 2. Theory

To understand the nature of water-mediated catalysis, we computed the intermolecular electronic density (ρ) and the corresponding reduced electronic density gradient (s or RDG). Following the work of Johnson et al.[13], we utilized this information on the electronic distributions to trace the non-covalent interactions (NCI) present among the reactants. As suggested by these authors, the electron density, when multiplied by the sign of $\lambda_2$, the second Hessian eigenvalue of the Laplacian of the electron density, can characterize the type of interaction. This value characterizes the strength of the interaction by means of the density and its curvature, thanks to the sign of the second eigenvalue. The interactions revealed by NCI correspond to both favourable and unfavourable interactions. The negative sign of $\lambda_2$ would indicate H-bonding, $\lambda_2 > 0$ the steric crowding, while near-zero to slight negative $\lambda_2$ would indicate the dispersion interaction. Integration of ρ in user-defined $\text{sign}(\lambda_2)\rho(r)$ ranges allows an estimation of the strength of NCIs in that specific range and takes the name of strength partitioning.

On the other hand, the topological analysis of the electron density ρ(r) yields atomic basins and QTAIM, Quantum Theory of Atoms in Molecules, atomic charges. Indeed, the integration of the electron density over the atomic basins, $\Omega_i$, provides the atomic population, $\overline{N}(\Omega_i)$, which is particularly important for the discussion of the bonding of the basin populations and the atomic charge, Q(A), by subtracting the atomic population from the atomic number.

In addition, the nature of chemical bonding is characterized by various properties of the electron density at critical points (CP). Many of these properties have been shown to correlate with experimental molecular properties. For example, QTAIM is useful for analyzing the nature of X-H - - - π interactions, where this theory shows that for all systems analyzed the bond paths correspond to preferable interactions[14], [15]. The electron density at the critical point, $\rho_{cp}$, has been shown on several occasions to be strongly correlated with the bond energies, and hence provides a measure of bond order[16].

The QTAIM CP for weak interactions corresponds to a minimum of the electron density in the normal direction of the interaction, which is a maximum in the orthogonal directions, and its curvature is designated as (3, -1) in the QTAIM notation. The nature of the chemical bond is characterized from various properties of the electron density at those CPs, especially the sign of the Laplacian of the electron density ($\nabla^2\rho_{cp}$) and the values of the kinetic energy density ($G_{cp}$), the potential energy density ($V_{cp}$), and the total energy density $H_{cp} = G_{cp} + V_{cp}$, following Bianchi's[17] and Macchi's classification[18].

Negative and positive values for the Laplacian of the electron density at the CP are assigned to "electron-shared" and "closed-shell" interactions, respectively. Moreover, based on the interpretation of $V_{CP}$ and $G_{CP}$ as the pressures exerted on and by the electrons at CP, Bianchi et al. distinguish three bonding regimes, depending on the value of the absolute ratio of the potential energy density to the kinetic energy density ($|V_{cp}|/G_{cp}$). The intermediate bond regime ($1 < |V_{cp}|/G_{cp} < 2$) lies between electron-shared covalent bonds (|Vcp|/Gcp greater than 2) and closed-shell ionic bonds or van der Waals interactions (|Vcp|/Gcp lower than 1) and includes dative bonds and ionic bonds of weak covalent character.

In the case of QTAIM studies on intra- and intermolecular interactions, the properties of critical points are most often analyzed. Particularly, for the D-H**...**A hydrogen bond, these are the characteristics of the H**...**A bond critical point; the electron density at H**...**A bcp, $\rho_{bcp}$, its Laplacian, $\nabla^2\rho_{bcp}$, the total electron energy density at bcp, $H_{bcp}$. When the Laplacian is negative, this implies a covalent character of the interaction and can therefore characterize covalent bonds as well as very strong hydrogen bonds. Indeed, Rozas *et al.* [14] proposed the classification of hydrogen bonds: weak and medium strength in hydrogen bonds show both positive $\nabla^2\rho_{bcp}$ and $H_{bcp}$ values, for

strong H-bonds, $\nabla^2\rho_{bcp}$ is positive and $H_{bcp}$ is negative and for very strong hydrogen bonds, $\nabla^2\rho_{bcp}$ and $H_{bcp}$ values are negative.

## 3. Calculation methods

The geometry of all systems was optimized at the MP2/cc-pvtz level, and the corresponding energies are given from a single point CCSD(T) calculation. In order to emphasize the effect of water alone on energy barriers the reaction energy barriers were not ZPE corrected. The GAUSSIAN09 series of program[19] was used for these calculations.

The electron density was subsequently analyzed with the AIMAll software[20], which implements Bader's Quantum Theory of Atoms in Molecules (QTAIM)[21], [22], and non-covalent interactions calculations were carried out with the NCIplot software[23] which is a program for calculating these interactions in molecular systems. Both QTAIM and NCIplot require a wfn file as input because they rely on the numerical representation of the wave function to extract information about the electronic structure and properties of the molecule. Gaussian software[19] was used to generate a wfn. The wfn file contains information about the electron density, wave function coefficients, and other properties that are necessary for these programs to perform their calculations and generate their output. QTAIM and NCI analysis were performed at the MP2/cc-pVTZ level. This level of calculation has already been used successfully on the same type of system[24].

## 4. Mechanism of the catalysis: example of ethylene.

In the reaction

$M + H^{\cdot} \rightarrow MH^{\cdot}$

a catalytic effect of a water molecule could be expected especially if the radical $H^{\cdot}$, neutral at infinite separation, undergoes more or less charge transfer with M when approaching this molecule. This way, it should acquire, nearby the TS region some charge $Q_H$, negative or positive. If $Q_H$ is negative the system can be stabilized by $H^{\cdot}\cdots$ H-OH interaction; if, on the contrary, $Q_H$ is positive, the system can be stabilized by $H^{\cdot}\cdots OH_2$ interaction.

The mechanism of such a catalytic effect will be detailed in the case of H addition to ethylene:

$H_2C{=}CH_2 + H^{\cdot} \rightarrow H_2C^{\cdot}\text{-}CH_3$

The evolution of electronic structure along the reaction coordinate (RC), and the resulting effect on the AIM charge $Q_H$ is displayed in Figure 1.

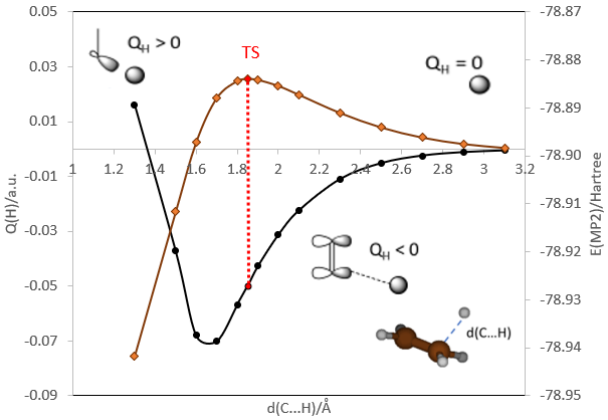


*Figure 1: Charge $Q_H$ (AIM, a.u.) of hydrogen atom as a function of d(C..H) distance (Å) in the H + $CH_2$=$CH_2$ addition reaction and energy evolution along the reaction pathway.*

At infinite C…H distance, the hydrogen atom is a neutral radical species. When the distance C..H decreases, a weak interaction with ethylene arises; it is dominated by a 3-electron π-H˙ interaction resulting in a weak electron transfer from ethylene to H and thus negative $Q_H$, especially nearby the TS (d(C…H) = 1.87 Å). When the C-H bond finally takes place, the H charge becomes positive.

Let us now consider the interaction of the H atom of this system with a water molecule. At infinite C…H separation, the interaction H…HOH is very weak, with a H…H distance ranging to ca. 3.1 to 3.9 Å according to the method[25] and an interaction energy of ca. 0.1 kcal/mol. On the contrary, nearby the TS, a stabilization of the system is expected by interaction of a positive hydrogen of water with negative hydrogen. We report in Figure 2 the H…HOH optimized distance as a function of the C…H in the $C_2H_4$…H…H-OH system.

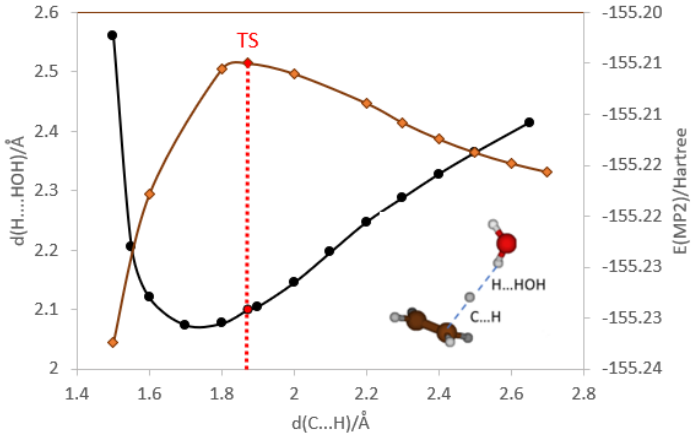


*Figure 2: Variation of the d(H…OH) distance as a function of d(C…H) in the H addition to $CH_2$=$CH_2$ in the presence of a water molecule and energy evolution along the reaction pathway.*

From this figure, we observe that H…HOH distance shortens when d(C…H) decreases, down to ca. 2.05 Å for a d(C..H) value of ca. 1.7 Å, which correspond of the greater negative charge of hydrogen

(Figure 1). A water molecule is thus able to stabilize the system selectively in the part of the RC close to the TS occurring at d(C…H) = 1.87 Å.

## 5. Catalytic effect of $H_2O$ in a panel of unsaturated molecules

The lowering of the energy barrier by a water molecule in the reaction

$M + H^{\cdot} \rightarrow MH^{\cdot}$

has been computed for M = $C_2H_4$, $C_2H_2$, CO, $H_2CO$, $H_2CS$, $H_2C=C=O$, $NH_2$-CH=$CH_2$ yielding respectively the radicals $CH_2^{\cdot}$-$CH_3$, $HC^{\cdot}=CH_2$, $HC=O^{\cdot}$, $H_3C$-$O^{\cdot}$, $H_3C=S^{\cdot}$, $H_3C$-$C^{\cdot}=O$ and $NH_2$-$CH^{\cdot}$-$CH_3$.

All M molecules are present in the interstellar space. The reaction is of particular importance for CO and $H_2CO$; it has been studied experimentally in the case of ketene[3]; aminoethene has been included to this panel as possessing a high energy π MO.

Two main primary mechanisms are usually considered for H addition to M on ice surface:

(i) The H atom reacts on the M molecule in interaction with ice:

$(ice)…M + H^{\cdot} \rightarrow (ice)…MH^{\cdot}$

(ii) The M molecule reacts on the H atom in interaction with ice:

$(ice)…H^{\cdot} + M \rightarrow (ice)…$ H-$M^{\cdot}$

Both mechanisms have been studied by Tieppo et al.[26] on M = CO and M = $H_2CO$ and it was found that reaction (ii) should be preferred to reaction (i). This prompted us to study the catalytic effect of a water molecule along the reaction path M + H…($H_2O$). It models the experimental situation in which ices submitted to cosmic rays yielding H atoms are bombarded by M molecules. Moreover, our aim was to compare the interactions of water with H in the TSs of H addition on carbon atom, from energetic and topological points of view, according to the nature of M and its intrinsic properties. For this purpose, the reaction path was constrained in order to prevent other possible interactions of $H_2O$…H with M, expected especially in systems containing CO and CS. Under this condition, the structures displayed in Figure 3 are nevertheless transition states, i.e. stationary points of first order.

In Table 1 are reported the activation energies in the absence ($E_a$) and in the presence ($E_a^w$) of $H_2O$, with respect to isolated M + H + $H_2O$.

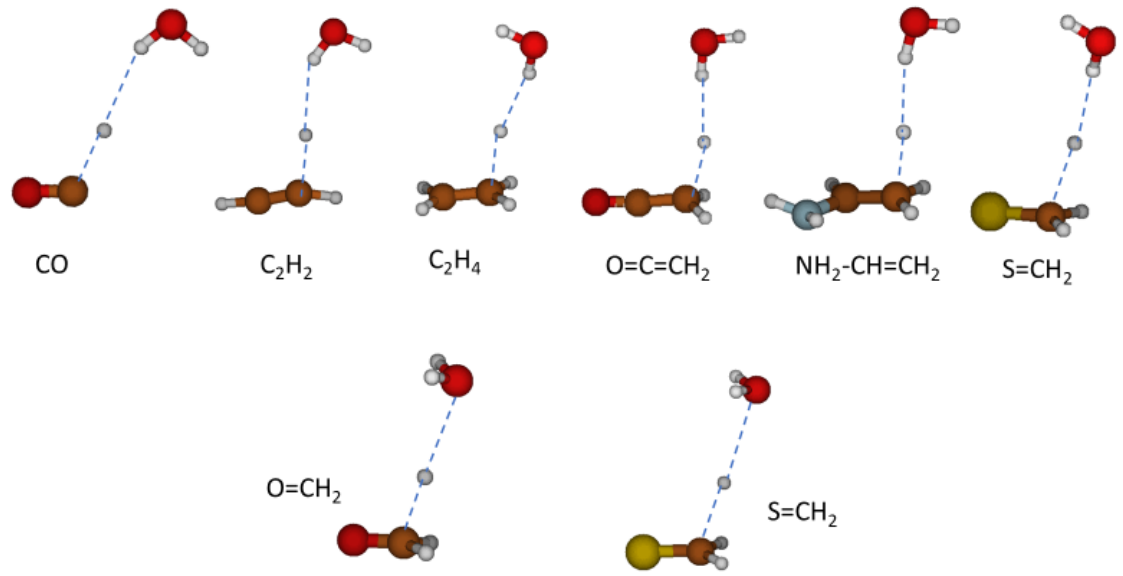


*Figure 3: Structure of TSs of H addition to carbon atom in some multiple bond molecules (see Table 1 for geometrical data).*

*Table 1: TS data in the H addition to multiple bonded carbon atom in the absence (M…H) and in the presence of $H_2O$ (M..H..HOH or M…H..$OH_2$): $Q_H$ QTAIM charge (a.u.) of H radical; d interactomic distances (Å, see also Fig.3); $E_a/E_a^w$ energy barriers in the absence/presence of water (kcal/mol)..*

| **M** | **M…H** | | | **M…H…HOH** | | | |
|---|---|---|---|---|---|---|---|
| | $Q_H$ | d(C….H) | $E_a$ | d(C….H) | d(H…..H) | $E_a^w$ | $E_a^w - E_a$ |
| **CO** | -0.001 | 1.742 | 3.38 | 1.742 | 2.32 | 2.77 | -0.61 |
| **$C_2H_2$** | -0.047 | 1.692 | 4.93 | 1.690 | 2.20 | 3.58 | -1.35 |
| **$C_2H_4$** | -0.050 | 1.859 | 2.83 | 1.872 | 2.10 | 1.47 | -1.36 |
| **$H_2C=C=O$** | -0.119 | 1.711 | 2.42 | 1.711 | 1.95 | 0.17 | -2.25 |
| **$NH_2$-CH=$CH_2$** | -0.104 | 1.854 | 1.03 | 1.881 | 1.96 | -1.52 | -2.55 |
| **$H_2C=S$** | 0.001 | 2.104 | 2.65 | 2.115 | 2.43 | 2.32 | -0.33 |
| | | | | | | | |
| | **M…H** | | | **M…H…$OH_2$** | | | |
| | $Q_H$ | d(C….H) | $E_a$ | d(C….H) | d(H….O) | $E_a^w$ | $E_a^w - E_a$ |
| **$H_2C=O$** | 0.060 | 1.650 | 4.94 | 1.673 | 2.455 | 3.55 | -1.36 |
| **$H_2C=S$** | 0.001 | 2.104 | 2.65 | 2.118 | 2.882 | 1.87 | -0.78 |

The difference $E_a^w - E_a$ is negative, meaning that the $E_a$ decreases in the presence of water, according to the nature of M the charge $Q_H$ in the M…H TS which varies in the range -0.119 to 0.060. This value depends on several parameters.

For CO, which has both low π and high π* MOs, the interaction with H is weak, $Q_H$ is near zero and a weak value of -0.61 kcal/mol is found for $E_a^w - E_a$.

Molecules $C_2H_4$, $C_2H_2$, $H_2C=C=O$ and $NH_2$-CH=$CH_2$ have a marked π-donor character, yielding $Q_H < 0$ which roughly decreases when the π MO energy increases, according to $C_2H_2 \approx C_2H_4 < CH_2=C=O <$

$NH_2$-CH=$CH_2$. In this series the lowering of $E_a$ by water ranges from -1.35 to -2.55 kcal/mol. The negative value of $E_a^w$ (-1.52 kcal/mol) for $NH_2$-CH=$CH_2$ corresponds to the CCDS(T) energy of a TS optimized at MP2 level. This point becomes lower than the isolated reactants, which means that a TS no longer exists.

On the other hand, $Q_H$ can become less negative or even positive by an additional interaction with a low energy empty MO of M. Indeed, methanal $H_2CO$ is a π-acceptor molecule resulting in a positive $Q_H$ value of 0.06 a.u. In this case, the TS is stabilized by interaction of $H^-$ with the oxygen nucleophilic site of $H_2O$, with a lowering of ca -1.36 kcal/mol of this TS.

Thiomethanal $H_2CS$ has a weak interaction with $H^-$, partly due to the long C…H distance of 2.1 Å in the TS, and partly to its weak electrophilicity. A very weak positive charge suggests a possible stabilization by M…H…$OH_2$ interaction. Indeed, the corresponding $E_a^w$ is found at 1.87 kcal/mol, -0.78 kcal/mol with respect to $E_a$. But the TS is also stabilized, in a lesser extent (-0.33 kcal/mol), by M…H…HOH interaction. One can remark that for CO, which has also a very weak $Q_H$, no TS is found with a OC…H…$OH_2$ interaction.

For a deeper understanding of the interactions occurring in the TS's, a topological analysis was performed.

## 6. Topological study

6.1 Non-covalent interactions (NCI)

Calculations were performed for both systems, with and without water. Figure 4 shows the graphs of sign($\lambda_2$)ρ vs s and NCI isosurfaces obtained using the NCIplot program. In all cases the low RDG blue peak with a negative value of $-0.06 < \text{sign}(\lambda_2)\rho < -0.02$ suggests the presence of an attractive non-covalent interaction.

Furthermore, the figure indicates that the complex with water has more RDG peaks than the system without water, suggesting the presence of more non-covalent interaction. Apart from the first peak, a green peak with a slightly negative value of sign($\lambda_2$)ρ ≈ -0.01 a.u. is visible, indicating the existence of a dispersion interaction. This peak is extremely sharp, such that the NCI surface and critical point basically coincide. The stabilization of the complex is confined mainly to the critical point itself.

The gradient isosurfaces are colored according to the corresponding values of sign($\lambda_2$)ρ. The color-coding of the isosurfaces indicates the strength of interaction. Blue isosurfaces with large and negative values of sign($\lambda_2$)ρ indicate attractive interactions, such as dipole-dipole or hydrogen

bonding. Red isosurfaces, corresponding to large and positive values of sign($\lambda_2$)ρ, indicate non-bonding interactions. Green isosurfaces with values close to zero indicate weak van der Waals interactions. The stronger set of attractive interactions, represented by blue density isosurfaces, can be localized between the hydrogen atom and the molecule. On the other hand, the green isosurfaces localized between the hydrogen atom and the water molecule are characteristic of a van der Waals interaction. Thus, it appears that the water molecule facilitates the reaction through a non-covalent interaction, which is identified as dispersive in nature due to the low density at the isosurface.

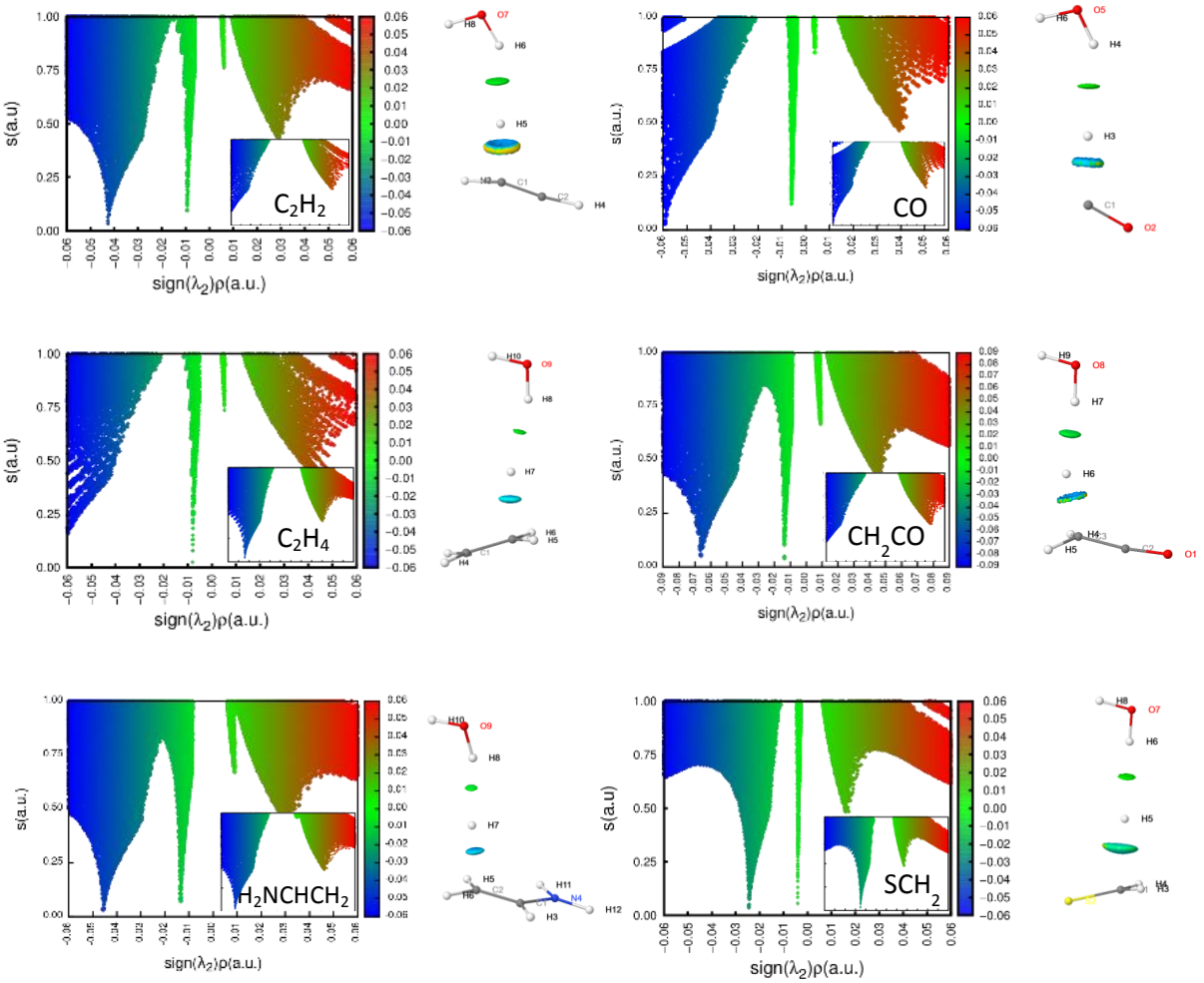


*Figure 4: Distribution of reduced density gradient (RDG) with respect to the electron density multiplied by the sign of second Hessian eigenvalue for both complexes (with water and without water for the "small" NCIplot) and NCI isosurfaces (s = 0.5 a.u.) for water-containing systems. A scale -0.06 < sign($\lambda_2$)ρ < 0.06 a.u. was used to colour the isosurfaces.*

## 6.2. QTAIM results

Table 2 shows that all QTAIM descriptors decrease with increasing HH distance, except for potential energy density ($V_{cp}$) and the total electron energy density ($H_{cp}$) decrease. More precisely the values of the electron density and its Laplacian at the critical point H...H increase inversely with the distance

between the two hydrogens due to the increasing orbital overlap. For all the complexes studied, the density Laplacian is positive at the critical point of the H...H interaction which means that the shared density of the bond in the bonding region is dominated by the positive kinetic energy ($G_{cp}$). The electron density is quite small (from $10^{-2}$ to $10^{-3}$ a.u. like in van der Waals complexes). At last, as expected [27]–[30], density and the Laplacian are strongly correlated with distance (Figure 5). Total electron energy density $H_{bcp}$ is positive in R= CO, $H_2CS$, $C_2H_4$ which characterizes a weak interaction but negative for the others (R= $H_2N$-CH=$CH_2$, $H_2C$=C=O), which indicates a stronger interaction as in the typical case of the strong hydrogen bond. The |V|/G ratio is less than 1.0 (Van der Waals type interaction according to Bianchi et al.[17]) except for the first two complexes in the table (referred to by Bianchi et al. as the intermediate bond regime). Finally, in Figure 6 we have plotted the evolution of the Laplacian as a function of the activation energy difference (ΔTS). We observe a good correlation between the two parameters (R=0.9589), confirming that the value of the Laplacian at the critical point of the HH interaction is a good criterion for assessing the activation barrier.

*Table 2: HH distance and QTAIM descriptors (in a.u.) at H…H critical point corresponding to the electron density ($\rho_{cp}$), Laplacian ($\nabla^2\rho_{cp}$), potential energy density ($V_{cp}$), kinetic energy density ($G_{cp}$), total energy density ($H_{cp}$), and ratio $|V_{cp}|/G_{cp}$ for transition state with water molecule.*

| R | d(H...H) | $\rho_{cp}/10^{-2}$ | $\nabla^2\rho_{cp}/10^{-2}$ | $V_{cp}/10^{-3}$ | $G_{cp}/10^{-3}$ | $H_{cp}/10^{-4}$ | $\lvert V_{cp}\rvert/G_{cp}$ |
|---|---|---|---|---|---|---|---|
| $H_2N$-CH=$CH_2$ | 1.96 | 1.3529 | 2.5645 | -7.6786 | 7.0449 | -6.3371 | 1.090 |
| $H_2C$=C=O | 1.95 | 1.3787 | 2.5199 | -7.7726 | 7.0361 | -7.3649 | 1.105 |
| $C_2H_4$ | 2.10 | 0.9372 | 2.1055 | -5.1218 | 5.1928 | 0.7102 | 0.986 |
| $C_2H_2$ | 2.20 | 0.8033 | 1.8037 | -4.1831 | 4.3462 | 1.6303 | 0.962 |
| CO | 2.32 | 0.5948 | 1.5008 | -3.0245 | 3.3882 | 3.6371 | 0.893 |
| $H_2CS$ | 2.43 | 0.4070 | 1.2221 | -1.9731 | 2.5142 | 5.4111 | 0.785 |

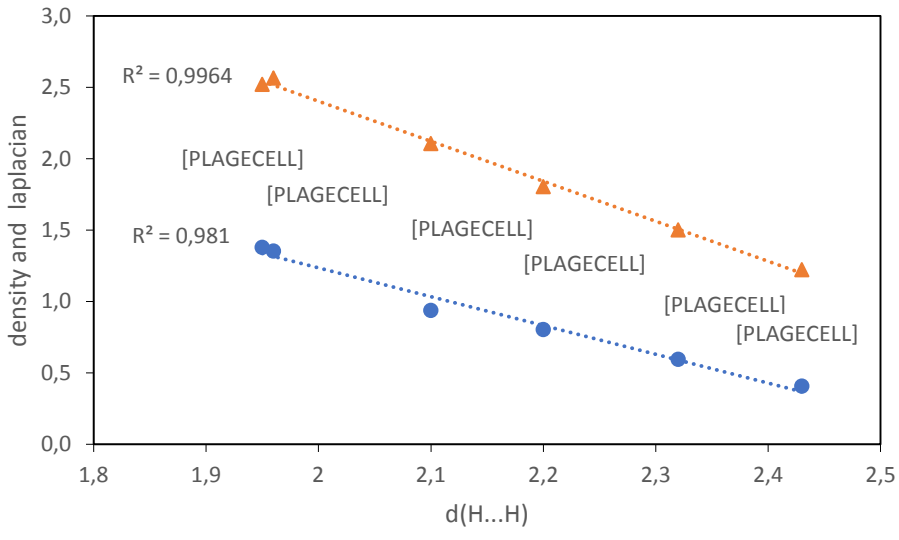

*Figure 5: $\rho_{CP}$ (dot points) and $\nabla^2\rho_{CP}$ (triangle points) vs d(H…H) (in a.u. and Å) for transition state with water molecule.*

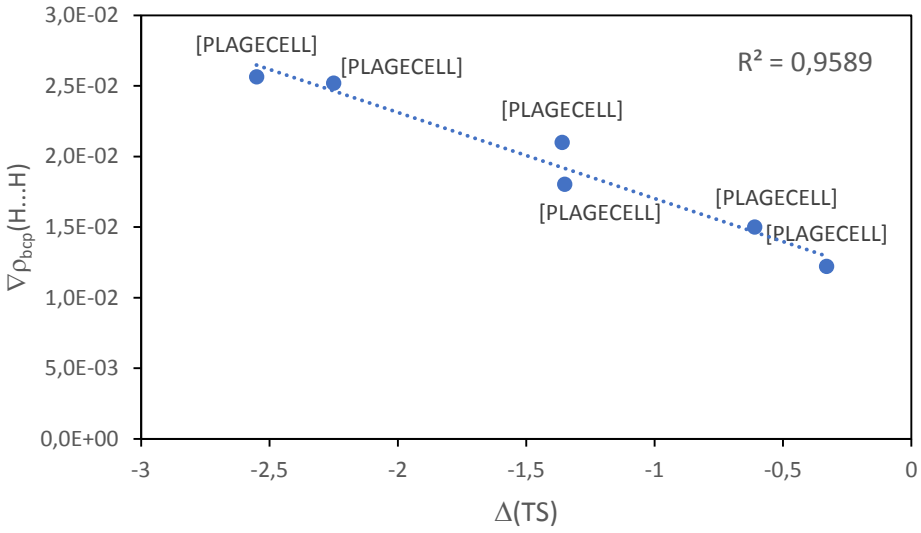


*Figure 6 : $\nabla^2\rho_{CP}$ vs $\Delta$TS (in e$Å^{-5}$ and Å, respectively) for transition state with water molecule.*

## 7 Catalytic effect of the $(H_2O)_2$ and $(H_2O)_3$ clusters

In the cluster $(H_2O)_2$ the hydrogen bond involves a weak charge transfer from one molecule to the other: as a result ( Figure 7), two hydrogen atoms are more positive than in $H_2O$, and one oxygen atom is more negative than in $H_2O$. One can thus assume that this cluster can interact more strongly than the monomer with H, according to its charge.

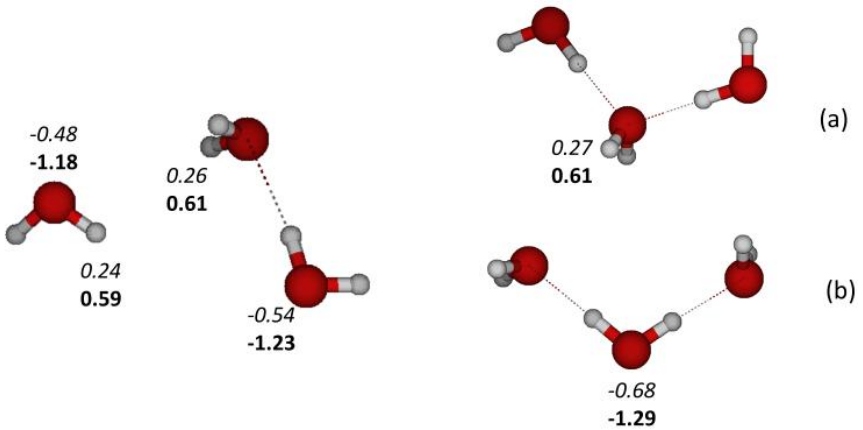


*Figure 7: Atomic charges of concern in some $(H_2O)_n$ (n=1, 2, 3) clusters; italic : Mulliken; bold: AIM.*

The various TS are shown in Figure 8. As in the case of a single water molecule, the geometry has been constrained to avoid parasitic interaction of water with M.

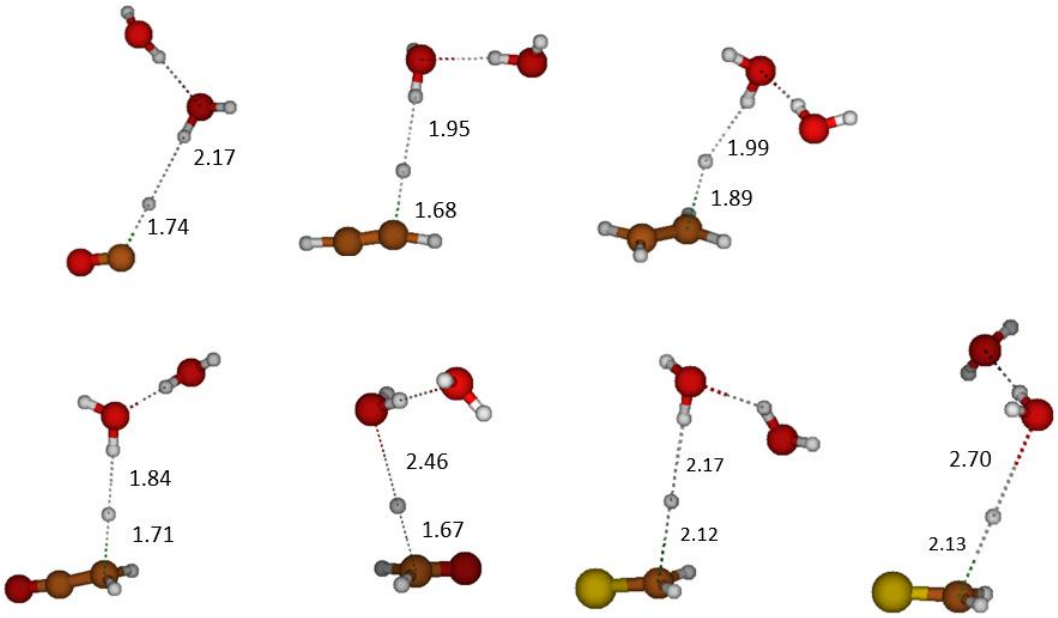


*Figure 8: TS structure for H addition to M in the presence of two water molecules.*

The activation energies $E_a^{2w}$ in the presence of two water molecules are displayed in Table 3, together with the variations of $E_a$ due to one ($E_a^{W} - E_a$) and a second ($E_a^{2W} - E_a^{w}$) water molecules.

*Table 3 Energy barrier $E_a^{2W}$ in the presence of 2 water molecules; respective decreases of the energy barrier by the first ( $E_a^{w} - E_a$) and the second ($E_a^{2W} - E_a^{w}$ ) water molecule.*

| M | $E_a^{2W}$ | $E_a^{w} - E_a$ | $E_a^{2W} - E_a^{w}$ |
|---|---|---|---|
| **CO** | 2.63 | -0.61 | -0.14 |
| **$C_2H_2$** | 2.85 | -1.35 | -0.73 |
| **$C_2H_4$** | 0.94 | -1.36 | -0.53 |
| **$H_2C=C=O$** | -0.77 | -2.25 | -0.93 |
| **$H_2C=O$** | 3.08 | -1.39 | -0.47 |
| **$H_2C=S$ (a)** | 2.11 | -0.33 | -0.20 |
| **$H_2C=S$ (b)** | 1.66 | -0.78 | -0.20 |

The effect of the second $H_2O$ molecule is smaller but significant: from 30 % to 60 % the effect of the first one, except for CO (20 %). In particular, we observe the vanishing of the activation energy for ketene $CH_2=C=O$.

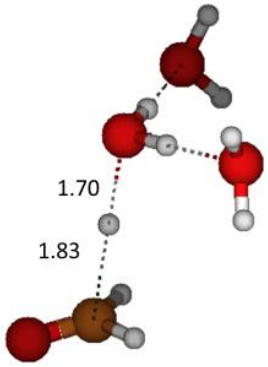


*Figure 9: TS structure of the H addition to $H_2CO$ in the presence of 3 water molecules.*

Dealing with $(H_2O)_3$ clusters, the maximum hydrogen atomic charge is expected to be found in structure (a) Figure 9 due to the attracting effect of two water molecules on the central one. But this increase is zero (AIM) or negligible (Mulliken). On the other hand, structure (b) possesses an oxygen atom significantly more negative than in $H_2O$ dimer. The corresponding TS of H addition on $H_2CO$ in the presence of a frozen $(H_2O)_3$ cluster is displayed in Figure 9, and is found at 2.63 kcal/mol above the sum of isolated $H_2CO$ + H + $(H_2O)_3$ energies. We summarize in Table 4 the effects of $(H_2O)_n$ on the TS of H + $H_2CO$ addition.

*Table 4: Energy barrier $E_a$ of H addition to $H_2CO$ in the presence of n water molecules.*

| n | 0 | 1 | 2 | 3 |
|---|---|---|---|---|
| $E_a$ | 4.94 | 3.55 | 3.08 | 2.63 |

## 8 Conclusion

We evidenced the catalytic effect of water molecules for H addition to double bonded carbon in a panel of seven molecules M. The lowering of the energy barrier ranges from ca. 20 % for CO to 100 % for ketene and aminoethane.

This effect originates from a double M...H...($H_2O$) interaction nearby the TS which was discussed by QTAIM and NCI approaches. The NCI results qualified both interactions, while the QTAIM results demonstrated the link between geometric and energetic parameters with topological descriptors. In this sense, we have demonstrated that the strength of the H...H interaction correlates strongly with the distance of this interaction, as well as with the difference in activation energies.

Though the reaction paths were in some extend constrained to allow a direct comparison of the various systems, they are close to the expected situation when ices submitted to cosmic rays are

bombarded by M molecules. Indeed, by water decomposition, hydrogen atoms are likely to be present on the surface, in weak interaction with water molecules of the bulk.

[1] The Cologne Database for Molecular Spectroscopy|CDMS, https://cdms.astro.uni-koeln.de/, (accessed October 13, 2023).
[2] T. Chiavassa, F. Borget, J.-P. Aycard, E. Dartois, L. d'Hendecourt, *Actual. Chim.*, **2005**, *283*, 12.
[3] M. Ibrahim, J.-C. Guillemin, P. Chaquin, A. Markovits, L. Krim, *Phys. Chem. Chem. Phys.*, **2022**, 24, 23245.
[4] A. Pérez-Villa, F. Pietrucci, A. M. Saitta, *Phys. Life Rev.*, **2020**, 33-35, 105.
[5] A. Germain, L. Tinacci, S. Pantaleone, C. Ceccarelli, P. Ugliengo, *ACS Earth Space Chem.*, **2022**, 6, 1286.
[6] V. Wakelam, J.-C. Loison, R. Mereau, M. Ruaud, *Mol. Astrophys.*, **2017**, 6, 22.
[7] A. Das, M. Sil, P. Gorai, S. K. Chakrabarti, J. C. Loison, *Astrophys. J. Suppl. Ser.*, **2018**, 237, 9.
[8] A. Rimola, D. Skouteris, N. Balucani, C. Ceccarelli, J. Enrique-Romero, V. Taquet, P. Ugliengo, *ACS Earth Space Chem.*, **2018**, 2, 720.
[9] J. Enrique-Romero, A. Rimola, C. Ceccarelli, P. Ugliengo, N. Balucani, D. Skouteris, *ACS Earth Space Chem.*, **2019**, 3, 2158.
[10] A. Rimola, M. Sodupe, P. Ugliengo, *Phys. Chem. Chem. Phys.*, **2010**, 12, 5285.
[11] A. Rimola, V. Taquet, P. Ugliengo, N. Balucani, C. Ceccarelli, *Astron. Astrophys.*, **2014**, 572, A70.
[12] S. Ferrero, L. Zamirri, C. Ceccarelli, A. Witzel, A. Rimola, P. Ugliengo, *Astrophys. J.*, **2020**, 904, 11.
[13] E. R. Johnson, S. Keinan, P. Mori-Sánchez, J. Contreras-García, A. J. Cohen, W. Yang, *J. Am. Chem. Soc.*, **2010**, 132, 6498.
[14] I. Rozas, I. Alkorta, J. Elguero, *J. Phys. Chem. A*, **1997**, 101, 9457.
[15] S. J. Grabowski, J. Leszczyński, *Chem. Phys.*, **2009**, 355, 169.
[16] R. J. Boyd, S. C. Choi, *Chem. Phys. Lett.*, **1986**, 129, 62.
[17] R. Bianchi, G. Gervasio, D. Marabello, *Inorg. Chem.*, **2000**, 39, 2360.
[18] P. Macchi, D. M. Proserpio, A. Sironi, *J. Am. Chem. Soc.*, **1998**, 120, 13429.
[19] M. J. Frisch, G. W. Trucks, J. R. Cheeseman, G. Scalmani, M. Caricato, H. P. Hratchian, X. Li, V. Barone, J. Bloino, G. Zheng, T. Vreven, J. A. Montgomery, G. A. Petersson, G. E. Scuseria, H. B. Schlegel, H. Nakatsuji, A. F. Izmaylov, R. L. Martin, J. L. Sonnenberg, J. E. Peralta, J. J. Heyd, E. Brothers, F. Ogliaro, M. Bearpark, M. A. Robb, B. Mennucci, K. N. Kudin, V. N. Staroverov, R. Kobayashi, J. Normand, A. Rendell, R. Gomperts, V. G. Zakrzewski, M. Hada, M. Ehara, K. Toyota, R. Fukuda, J. Hasegawa, M. Ishida, T. Nakajima, Y. Honda, O. Kitao, H. Nakai, Gaussian 09. .
[20] T. A. Keith, AIMAll (Version 17.11.04). .
[21] R. F. W. Bader, *Chem. Rev.*, **1991**, 91, 893.
[22] R. F. W. Bader, *Acc. Chem. Res.*, **1985**, 18, 9.
[23] J. Contreras-García, E. R. Johnson, S. Keinan, R. Chaudret, J.-P. Piquemal, D. N. Beratan, W. Yang, *J. Chem. Theory Comput.*, **2011**, 7, 625.
[24] M. Boland, P. Chaquin, F. Volatron, A. Markovits, *Astron. Astrophys.*, **2024**, 682, A13.
[25] A. N. Alexandrova, *J. Phys. Chem. A*, **2010**, 114, 12591.
[26] N. Tieppo, F. Pauzat, O. Parisel, Y. Ellinger, *Mon. Not. R. Astron. Soc.*, **2023**, 518, 3820.
[27] I. Alkorta, L. Barrios, I. Rozas, J. Elguero, *J. Mol. Struct. THEOCHEM*, **2000**, 496, 131.
[28] E. Espinosa, M. Souhassou, H. Lachekar, C. Lecomte, *Acta Crystallogr. B*, **1999**, 55, 563.
[29] A. M. Pendás, A. Costales, V. Luaña, *J. Phys. Chem. B*, **1998**, 102, 6937.
[30] I. Alkorta, I. Rozas, J. Elguero, *Struct. Chem.*, **1998**, 9, 243.